

**This item is the archived peer-reviewed author-version of:**

A simple evaluation procedure for range camera measurement quality

**Reference:**

Bogaerts Boris, Penne Rudi, Sels Seppe, Ribbens Bart, Vanlanduit Steve.- A simple evaluation procedure for range camera measurement quality

Advanced concepts for intelligent vision systems : 17th International Conference, ACIVS 2016, Lecce, Italy, October 24-27, 2016, Proceedings / Blanc-Talon, Jacques [edit.]; et al. - ISSN 0302-9743 - Springer International Publishing, 2016, p. 286-296

Full text (Publishers DOI): [http://dx.doi.org/doi:10.1007/978-3-319-48680-2\\_26](http://dx.doi.org/doi:10.1007/978-3-319-48680-2_26)

# A simple evaluation procedure for range camera measurement quality

Boris Bogaerts<sup>1</sup>, Rudi Penne<sup>1,2</sup>, Seppe Sels<sup>1</sup>, Bart Ribbens<sup>1</sup>, and Steve Vanlanduit<sup>1</sup>

<sup>1</sup> Faculty of Applied Engineering, University of Antwerp, Groenenborgerlaan 171, B-2020 Antwerp, Belgium.

<sup>2</sup> Department of Mathematics, University of Antwerp, Belgium.  
`boris.bogaerts@uantwerpen.be`

**Abstract.** Range cameras suffer from both systematic and random errors. We present a procedure to evaluate both types of error separately in one test. To quantify the systematic errors, we use an industrial robot to provide a ground truth motion of the range sensor. We present an error metric that compares this ground truth motion with the calculated motion, using the range data of the range sensor. The only item present in the scene is a white plane that we move in different positions during the experiment. This plane is used to compute the range sensor motion for the purpose of systematic error measurement, as well as to quantify the random error of the range sensor. As opposed to other range camera evaluation experiments this method does not require any extrinsic system calibration, high quality ground truth test scene or complicated test objects. Finally, we performed the experiment for three common Time-of-flight (TOF) cameras: Kinect One, Mesa SR4500 and IFM 03D303 and compare their performance.

**Keywords:** Range camera, Hand-eye transformation, Time-of-flight, Error metric

## 1 Introduction

In this paper we present an easy procedure to quantify both the systematic and random errors of range sensors. Consequently, the presented method provides an evaluation tool to compare different range sensors. The proposed test delivers quantitative error values, that are easy to compare.

We distinguish between random and systematic errors, because different tasks are sensitive to different types of error. For example, the recognition of CAD objects in a scene is sensitive to random noise. Indeed, the presence of noise is a serious obstacle for segmentation [13]. On the other hand, applications of range sensors that make use of plane features, are sensitive to systematic errors. For example, in order to determine the eigenmotion of a Time-of-flight TOF camera by means of plane measurements [9, 4], random noise can be handled by robust plane fitters [16], but the calculation of the transformation depends on

the quality of the plane coordinates. Systematic errors induce inaccuracies in these determined plane coordinates, which in turn result in a deterioration in the quality of the determined camera motion.

Other experiments designed to evaluate various errors of range sensors rely on very strict manual placement [2] or calibration (relative to ground truth) of the range sensor [15, 7]. Both these methods are cumbersome and affect the estimate of this error. Some experiments require detailed knowledge about the measurement scene [15, 7], and require an extra highly accurate range scanner. Our method does not rely on extra system calibrations or ground truth scenes.

The presented test method comprises experiments with TOF cameras (as an example of range sensors) rigidly attached to a robot manipulator (Fig. 1). This choice was motivated by the reliability of the current robot controllers, such that the motion of the robot's end effector can be considered as an accurate ground truth. The ground truth motion of the robot manipulator will be compared with the motion determined by the range sensor to evaluate systematic errors of the sensor.

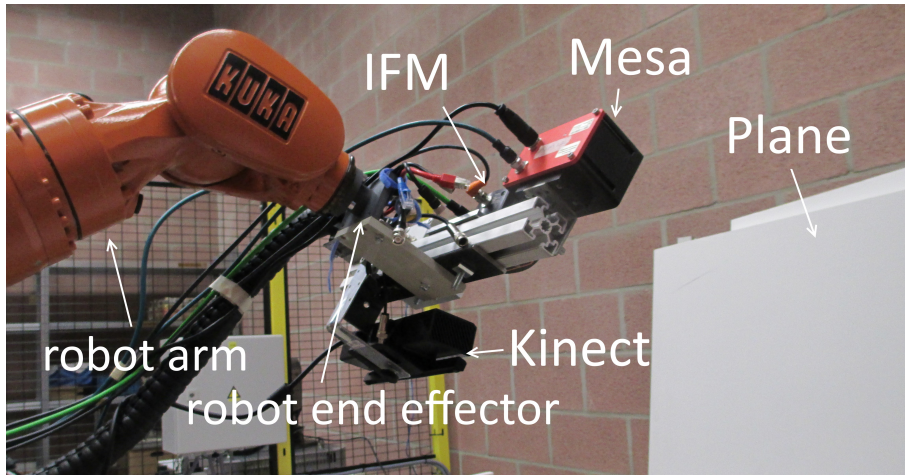


**Fig. 1.** Measurement setup. An industrial robot Kuka KR16W is holding the three ToF cameras we compared: Kinect One, Mesa SR4500 and IFM 03D303. The scene also contains a white plane.

However, it is a challenge to have access to this ground truth data, because of the famous hand-eye calibration problem [14]. This problem is caused by the fact that the relative motion between two positions of the camera is known in the robot basis instead of the camera basis. The transformation matrix between both reference frames, one at the camera center and the other at the robot tool center, is unknown. We can solve for this transformation matrix by doing the

hand-eye calibration [8, 14], but this is based on the availability of a reliable camera transformation. Therefore, using the hand-eye calibration for evaluating the systematic errors of a range sensor (camera motion) gives rise to a conceptual loop, and hence is not desirable. However, the quality of the system of equations that solves this hand-eye calibration will serve as an indication for the degree of systematic error: the *hand-eye error metric* (Section 3.2).

The second central element in our experiment is a planar object that is present in the scene. This plane has two functions. On one hand, the transformation of the range camera can be estimated using different orientations of this plane; the systematic error behaviour of the range sensor will be evaluated by means of the quality of the computed transformation. On the other hand, the noise of measurements on these planes is used to characterize random error. This approach yields a decoupled evaluation tool. Indeed, the plane based method for computing the motion of the sensor does not introduce random errors, while the effect of random errors on the estimated plane coordinates is very low.

The experiment consists of 4 steps:

1. Mount the range camera on the robot (no special pose is required).
2. Define a number of preprogrammed positions, allowing the attached camera to view a given plane (flat surface).
3. Capture a point cloud at each of the preprogrammed positions, corresponding to the viewed plane.
4. Repeat step 3 for at least three configurations of the measurement plane. It is important that the camera is rigidly attached to the robot, excluding relative motion of this camera with respect to the robot during the entire experiment.

## 2 Experimental setup

The objective of our experiments is to measure both the systematic and random measurement errors of range cameras. We have tested and compared three common Time-of-flight cameras: **Kinect One**, **Mesa SR4500** and **IFM 03D303**. In order to compare the computed motion to a reliable ground truth, the TOF sensors are mounted rigidly on an articulated robotarm (KUKA KR16W, with a repeatability error less than 0.1mm) as shown in Fig. 1. In each single test we consider TOF images for a pair of robot positions, in which the attached camera observes a fixed plane. During the whole experiment we arranged five distinct positions of this plane, that could be viewed from twenty preprogrammed robot configurations, providing a supply of  $\binom{20}{2}$  test pairs for each camera.

For the evaluation we need sets of 3-D points, generated by the TOF sensors, directly provided in  $(X, Y, Z)$  coordinates with respect to the camera frame. This means that we assumed a priori calibrated TOF cameras.

We only use points on the viewed planar object in the experimental setup. To this end we automatically selected the pixels in the white board that is visible in every TOF frame.

Next, we compute the best-fitting plane supporting the reconstructed 3-D points in all given range images of the fixed board. Working with plane coordinates provides following advantages over classical point based methods ([18, 1, 3]):

1. A fitted plane reduces error fluctuations compared to 3-D point measurements.
2. There is no need to detect point features and to establish correspondences between them.
3. It is easy to find a set of viewpoints from which a part of the plane is visible.
4. It is not necessary that the calibration object (in this case a board) is entirely visible in each used viewpoint.

This best-fitting plane can be computed by *principal component analysis*, but we prefer a more robust estimate based on Ransac [5]. More precisely, we applied the Matlab function `pcfitplane`, that implements the algorithm of [16]. Ransac eliminates pixels that exceed a predetermined threshold from the fitted model, even if they were selected inside the measured plane. To determine the random noise relative to the measured plane we use the fitted plane to determine the borders of the plane in the image, and calculate the total deviation of all pixels inside this segmented planar region with respect to the fitted plane.

### 3 Evaluation metric for systematic error

The goal of this section is to devise an error metric that is a measure for the dimensional accuracy of a range sensor. There are two difficulties that need to be tackled:

1. The error metric should be independent of measurement noise. This is because we want to assess random error and systematic error independently.
2. The robot motion cannot be used directly as ground truth. This is because there is an unknown transformation between the robot tool center and the range sensor. This transformation is called the hand-eye transformation.

The first problem will be tackled by estimating the motion of the range camera by using planes. To get around the second problem we use an error metric we call the *hand-eye error metric*.

#### 3.1 Plane-based method to estimate the motion of a range camera

A common way to describe mathematically the rigid motion of a TOF camera or any other 3-D object is by means of the coordinate transformation between the two positions of a rigidly attached reference frame before and after the motion. The rotational part of the rigid motion is represented by a  $3 \times 3$  orthonormal matrix  $R$  ( $R^{-1} = R^T$ ), and the translation part by a  $3 \times 1$  vector  $t$ . If  $p$  and  $p'$

are the  $3 \times 1$  coordinate vectors of a given spatial point w.r.t. the rigidly attached reference frame before and after the motion respectively, then

$$p = R \cdot p' + t. \quad (1)$$

Often, it is convenient to represent this transformation by one matrix multiplication  $\bar{p} = B \cdot \bar{p}'$ , using homogeneous coordinates  $\bar{p} = (p^T, 1)^T$  with weight 1, and a  $4 \times 4$  transformation matrix

$$B = \begin{pmatrix} R & t \\ \mathbf{0}^T & 1 \end{pmatrix} \quad (2)$$

with  $\mathbf{0}$  the  $3 \times 1$  zero vector.

If the rigid transformation of a depth camera is represented by a 4 by 4 transformation matrix  $B$  acting on homogeneous coordinates of 3-D points as given by Eqn. 2, then the corresponding dual transformation acting on plane coordinates  $(a, b, c, d)^T$  is represented by  $B^{-T}$  [11]:

$$\bar{p} = B \cdot \bar{p}' \Leftrightarrow \begin{pmatrix} a \\ b \\ c \\ d \end{pmatrix} \sim B^{-T} \begin{pmatrix} a' \\ b' \\ c' \\ d' \end{pmatrix} \Leftrightarrow \begin{pmatrix} a' \\ b' \\ c' \\ d' \end{pmatrix} \sim B^T \begin{pmatrix} a \\ b \\ c \\ d \end{pmatrix} \quad (3)$$

Because the homogeneous plane coordinates  $(a, b, c, d)^T$  are determined up to a scale factor, it is convenient to normalize the plane normals  $n = (a, b, c)^T$  to length 1. This leaves us with one more ambiguity, due to the two opposite directions for  $n$ . This can be resolved by some additional constraint, e.g. requiring that all plane normals point towards the 3D sensor. With these conventions the proportional similarity of Eqn. 3 can be replaced by an equality. Due to the normalization of the plane coordinates, the transformation between planes can be computed analogous to the rigid transformation between points. For example, the least squares algorithm of [1] can be used. For more details on the implementation with planes, we refer to [17, 12, 4].

### 3.2 The hand-eye error metric

We evaluate the depth performance of a range sensor by the correctness of the reconstructed planes (white boards). On its turn, the reconstruction of the planes is validated by the accuracy of the computed motion between two camera positions. The estimated camera motion can be compared with the known motion of an articulated robot arm the camera was rigidly attached to (Fig. 1). However, the camera motion is *conjugated* to the known robot motion. This means that the motion is the same, but expressed in different bases. If the  $4 \times 4$  transformation matrix  $A$  denotes the motion of the robot, and if  $B$  represents the camera motion matrix, then this conjugacy is algebraically expressed by *similarity* of matrices [6]:

$$A = XBX^{-1} \quad (4)$$

In the literature this issue is also known as the  $AX = XB$  calibration problem [8]. This  $4 \times 4$  matrix  $X$  is the so-called *hand-eye calibration* between robot and camera. In general, the transformation  $X$  between the robot coordinate frame and the camera frame is not a priori known. In our validation experiments, the robot transformation  $A$  is accurately known and considered as ground truth, while the computation of  $B$  has to be validated for the different types of TOF cameras. To this end, we compose a system of linear equations in the unknown entries of the hand-eye matrix  $X$ , following [8]. For the convenience of the reader we briefly explain how this system of equations is obtained.

If the exact camera transformation  $B$  matrix is available then we are guaranteed to have a solution  $X$  to the hand-eye calibration problem

$$AX - XB = 0 \quad (5)$$

These matrices are all  $4 \times 4$  transformation matrices and can be expressed as in Eqn. 2:

$$\begin{pmatrix} R_A & t_A \\ \mathbf{0}^T & 1 \end{pmatrix} \begin{pmatrix} R_X & t_X \\ \mathbf{0}^T & 1 \end{pmatrix} = \begin{pmatrix} R_X & t_X \\ \mathbf{0}^T & 1 \end{pmatrix} \begin{pmatrix} R_B & t_B \\ \mathbf{0}^T & 1 \end{pmatrix}. \quad (6)$$

After performing the matrix multiplication, the resulting block matrix can be decoupled into the following system of matrix equations:

$$\begin{cases} R_A R_X = R_X R_A \\ R_A t_X + t_A = R_X t_B + t_X \end{cases} \Leftrightarrow \begin{cases} R_A R_X - R_X R_A = 0 \\ R_X t_B + (I_3 - R_A)t_x = t_A \end{cases} \quad (7)$$

The *tensor product*  $\otimes$  of matrices appears to be a convenient tool to rearrange the factors of a matrix product in order to separate the unknown matrix in a matrix equation [10]:

$$M \cdot P \cdot N = Q \Leftrightarrow (N^T \otimes M)\text{vec}(P) = \text{vec}(Q), \quad (8)$$

where  $\text{vec}(Q)$  denotes the *vectorization* of matrix  $Q$ : the vector obtained by concatenating the columns of  $Q$ . Consequently, using Eqn. 8, we can reformulate Eqn. 7 as follows:

$$\begin{cases} (I_3 \otimes R_A)\text{vec}(R_X) = (R_B^T \otimes I_3)\text{vec}(R_X) \\ (t_B^T \otimes I_3)\text{vec}(R_X) + (I_3 - R_A)t_X = t_A \end{cases} \quad (9)$$

yielding a system of twelve linear equations in the nine unknowns  $(\text{vec}(R_X)^T, t_X^T)$ :

$$M \cdot \begin{pmatrix} \text{vec}(R_X) \\ t_X \end{pmatrix} = s \Leftrightarrow \begin{pmatrix} I_3 \otimes R_A - R_B^T \otimes I_3 & 0 \\ t_B^T \otimes I_3 & I_3 - R_A \end{pmatrix} \begin{pmatrix} \text{vec}(R_X) \\ t_X \end{pmatrix} = \begin{pmatrix} \mathbf{0} \\ t_A \end{pmatrix} \quad (10)$$

Eqn. 10 was mentioned in the review paper [14] on hand-eye calibration. In order to determine  $(R_X, t_X)$  we need to know the robot motion  $A$  and the corresponding measured camera transformation  $B$ . To actually solve this system, at least three given transformation pairs  $(A, B)$  are necessary. Furthermore, to guarantee full rank for this system of equations the vectorized rotation matrices of the three given transformations must be linearly independent.

In practice, coping with noisy measurements, the camera motion  $B$  obtained from the plane-based method of Section 3.1 is not exact. Therefore, we combine Eqn. 10 for multiple transformation pairs  $(A_i, B_i)$  ( $1 \leq i \leq n$ ,  $n \geq 3$ ) as follows:

$$\begin{pmatrix} M_1 \\ \vdots \\ M_n \end{pmatrix} \begin{pmatrix} \text{vec}(R_X) \\ t_X \end{pmatrix} = \begin{pmatrix} s_1 \\ \vdots \\ s_n \end{pmatrix} \quad (11)$$

with

$$M_i = \begin{pmatrix} I_3 \otimes R_{A_i} - R_{B_i}^T \otimes I_3 & 0 \\ t_{B_i}^T \otimes I_3 & I_3 - R_{A_i} \end{pmatrix}, \quad s_i = \begin{pmatrix} \mathbf{0} \\ t_{A_i} \end{pmatrix} \quad (12)$$

The hand-eye transformation  $X$  can be estimated by the least-squares approximation (LSA) of this overdetermined system of linear equation. In our context, the estimation of  $X$  in itself is less important than the least-squares error of the LSA, because this indicates the quality of the system of equations, and hence it validates the accuracy of  $B$ . This motivates us to define the mean least-squares solution error of the LSA of this systems as an error metric for the depth sensor that provided the reconstruction of the planes, called the *hand-eye error metric (HEE)*.

$$HEE = \sqrt{\|s - M(M^T M)^{-1} M^T s\|^2 / (12n)} \quad (13)$$

with  $M = (M_1^T, \dots, M_n^T)^T$  and  $s = (s_1^T, \dots, s_n^T)^T$ . The error metric provided by Eqn. 13 is motivated by the following arguments:

- The robot transformation  $A$  is known accurately (we can assume zero noise for  $A$ ).
- The transformation matrix  $X$  necessarily exists and is fixed for a given robot-sensor system. Therefore, the hand-eye error would be zero if the rigid motion  $B$  of the depth sensor was computed correctly.
- HEE is able to assess the validity of a method over multiple measurements, yielding a growing system of equations (Eqn. 11). The ability to combine multiple camera positions in one error metric enables us to cover the whole image space of the range sensor, such that the complete sensor is evaluated.

## 4 Evaluation metric random error

The proposed experimental setup allows us to measure the random noise of the tested camera simultaneously. Different planes are measured in the scene in order to compute the transformation of the range sensor between different robot positions (Section 3.1). These planes are segmented by means of Ransac. With the computed plane coordinates it is possible to compute an expected depth measurement for each pixel inside the segmented rectangular image region representing the measured plane. The difference between the plane and the true depth measurements represents the measurement noise. The standard deviation

of the Euclidean distances between the 3D-reconstructed pixel and the fitting, characterizes the random noise of the tested range sensor.

Furthermore, during the proposed procedure, the plane is viewed from different directions. This allows us to evaluate the measurement noise as a function of the measurement angle (Figure 3).

## 5 Results

In the validation experiments described below, random transformations are sampled from our dataset. This dataset consists of measurements from twenty different robot positions. In each position, five images have been taken by a TOF sensor that was rigidly attached to the articulated robot arm. These TOF images contain 3-D point clouds from the scene. Finally, all these measurements have been repeated for three different commonly used Time-of-flight cameras: Kinect One, Mesa SR4500 and IFM O3D303. Both the systematic and random errors are evaluated separately:

1. For the systematic error, two random robot positions are chosen. The transformation of the range sensor between these positions is calculated using plane coordinates of the five planes measured in both positions. This random selection of positions is repeated fifteen times, avoiding to duplicate a previously chosen pair of transformations. Next the hand-eye error metric is calculated using these transformations (translations are in mm). The calculation of this error metric is repeated twenty times for different random positions. The distribution of this error metric is visualized for each TOF camera by means of a boxplot (Fig. 2).
2. For the evaluation of the random error, all measured planes are used. For each frame the standard deviation of the Euclidean distance between each measured point and the determined plane inside the segmented region represents the noise level. In addition, this noise level is plotted in Fig. 3 against the angle between the plane normal and the focal axis of the range sensor. The possible presence of a linear relation between the random error and the measurement angle is checked by the correlation coefficient.

### 5.1 Systematic error

Figure 2 shows the boxplots representing the distribution of the hand-eye error metric (HEE) for multiple different systems of selected transformations for three different sensors. A small HEE indicates a low systematic error. Indeed, in this case the hand-eye calibration, found as solution of the system of equations (11), is stable and hardly affected by the choice of transformations that contribute to this system. Furthermore, if the 3D calibration of the range camera is accurate, we expect the HEE metric to be the same for every included transformation. A large spread of the hand-eye error metric points toward unreliable estimates for the transformation of the camera. This unreliability indicates a change of systematic error across the measurement volume of the considered range sensor.

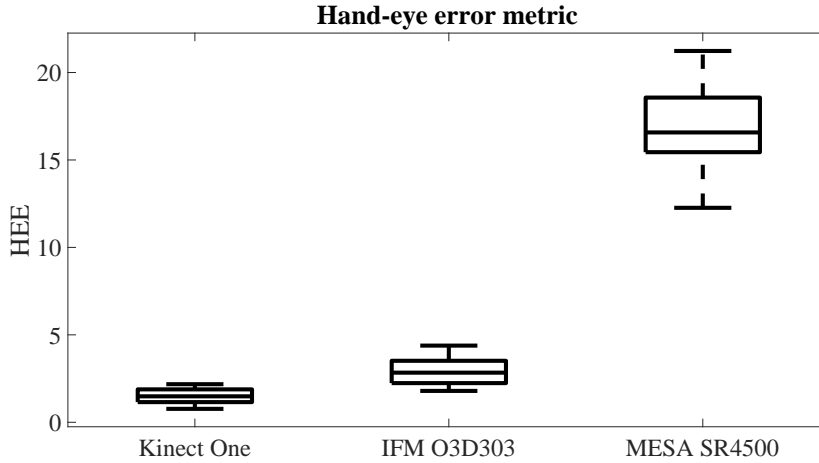


**Fig. 2.** Distribution of the hand-eye error metric for three different TOF cameras (transformations are in mm): Kinect One (mean: 0.92), IFM O3D303 (mean: 1.60) and Mesa SR4500 (mean: 5.59) represented as boxplot. This test shows that the systematic error of the Kinect One is low compared to the Mesa SR4500. The systematic error of the IFM O3D303 lies somewhere in between.

The test shows that the systematic error of the Kinect One is the lowest, followed by the IFM O3D303 while the Mesa SR4500 performs worst. This test indicates that the dimensional accuracy is the most reliable for the Kinect One.

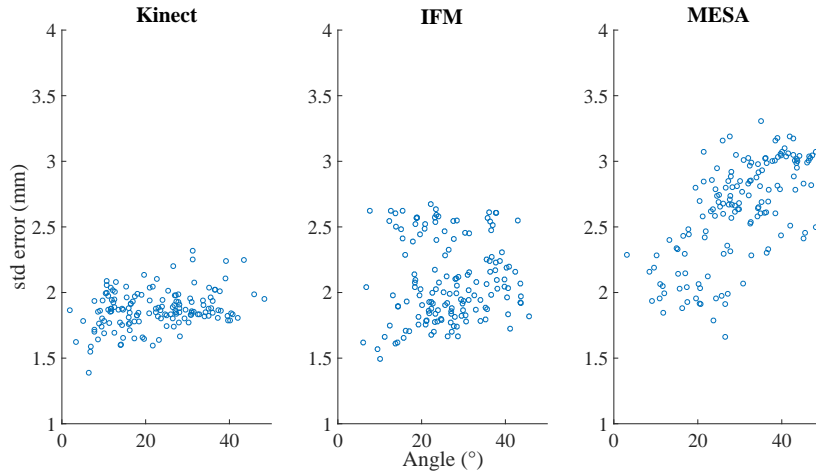
## 5.2 Random error

Figure 3 shows a scatter plot of the spread of the measurement error against the measurement angle. A low spread indicates a low noise level of the sensor. A possible linear relationship between the measurement angle and the noise level is evaluated by means of the correlation coefficient, because this would indicate that noise levels depend on the measurement angle.

The boxplots in Figure 3 show that the noise levels of Kinect One are the lowest. The noise levels of IFM O3D303 are the highest for small angles, but for larger angles (above 30 degrees) the noise level of MESA SR4500 becomes the highest. This is because there is a strong linear relationship between noise and angle for the MESA SR4500 (correlation coefficient of 0.67) but not for the IFM O3D303.

## 6 Conclusions

We presented a relatively simple experiment to compare different range sensors, both in terms of systematic and random measurement error. The experiment



**Fig. 3.** Scatter of the standard error against measurement angle for the three considered TOF cameras. Lower noise is better, and independence between measurement angle and measurement noise is desired. The correlation coefficients between the measurement angle and the measurement error for Kinect One, IFM O3D303 and MESA SR4500 are respectively: 0.29, 0.03 and 0.67

uses a robot and a plane. This robot is used to provide an accurate ground truth motion independent of the considered range sensor. Other methods to obtain an accurate ground truth motion are also allowed. This could for example be a coordinate measuring arm, infrared tracker, etc.

The data provided by this experiment contain useful characteristics of the considered range camera. The systematic error of the camera can be quantitatively assessed using the hand-eye metric. This error metric compares the ground truth motion with the motion assessed by the range camera. If both motions agree, this error metric is low. The noise levels can be assessed by computing the standard deviation of the difference between measured plane values and the plane fitted by a robust plane fitter. Because the measurement plane is viewed from different directions, we can determine the sensitivity of the measurement noise to the measurement angle, which is important in many applications.

This experiment can also be repeated to study different range sensor specific errors. For example, for a Time-of-flight camera the noise levels are dependent on the integration time. The test proposed in this paper can be repeated for different values of the integration time. The results provide insight in how the changed parameter affects both the systematic and random error.

## Acknowledgements

The first author holds a PHD grant from the research Fund-Flanders (FWO Vlaanderen). This research has also been funded by the government agency

Flanders Innovation & Entrepreneurship (VLAIO) by the support to the TETRA project Smart data clouds with project number 140336 and the Research Council of University of Antwerp (Stim-KP 31128 & the Research Committee of the Faculty of applied engineering fti-OZC).

## References

1. K. S. Arun, T. S. Huang, and S. D. Blostein. Least-squares fitting of two 3-d point sets. *9*(5):698–700, 1987.
2. Andrea Corti, Silvio Giancola, Giacomo Mainetti, and Remo Sala. A metrological characterization of the Kinect V2 time-of-flight camera. *Robotics and Autonomous Systems*, 75:584–594, 2016.
3. D.W. Eggert, A. Lorusso, and R.B. Fisher. Estimating 3-d rigid body transformations: a comparison of four major algorithms. *Machine Vision and Applications*, 9(5):272–290.
4. E. Fernández-Moral, J. González-Jiménez, P. Rives, and V. Arévalo. Extrinsic calibration of a set of range cameras in 5 seconds without pattern. In *International Conference on Intelligent Robots and Systems*. IEEE/RSJ, sep 2014.
5. M. Fischler and R. Bolles. Random sampling consensus: A paradigm for model fitting with applications to image analysis and automated cartography. *Communications of the ACM*, 24:381–385, 1981.
6. K. Hoffman and R.A. Kunze. *Linear algebra*. Prentice-Hall mathematics series. Prentice-Hall, 1971.
7. Kouros Khoshelham and Sander Oude Elberink. Accuracy and resolution of kinect depth data for indoor mapping applications. *Sensors*, 12(2):1437–1454, 2012.
8. J. Mao, X. Huang, and L. Jiang. A flexible solution to  $ax=xb$  for robot hand-eye calibration. In *Proceedings of the 10th WSEAS International Conference on Robotics, Control and Manufacturing Technology, ROCOM'10*, pages 118–122, Stevens Point, Wisconsin, USA, 2010. World Scientific and Engineering Academy and Society (WSEAS).
9. K. Pathak, A. Birk, N. Vaškevičius, and J. Poppinga. Fast registration based on noisy planes with unknown correspondences for 3-d mapping. *Trans. Rob.*, 26(3):424–441, June 2010.
10. K. B. Petersen and M. S. Pedersen. *The Matrix Cookbook*. Technical University of Denmark, nov 2012. Version 20121115.
11. H. Pottmann and J. Wallner. *Computational Line Geometry*. Springer-Verlag New York, Inc., Secaucus, NJ, USA, 2001.
12. C. Raposo, J.P. Barreto, and U. Nunes. Fast and accurate calibration of a kinect sensor. In *International Conference on 3D Vision*. IEEE, 2013.
13. S. Sels, B. Ribbens, B. Bogaerts, J. Peeters, and S. Vanlanduit. 3d model assisted fully automated scanning laser doppler vibrometer measurements. Submitted.
14. M. Shah, R. D. Eastman, and T. Hong. An overview of robot-sensor calibration methods for evaluation of perception systems. In *Proceedings of the Workshop on Performance Metrics for Intelligent Systems, PerMIS '12*, pages 15–20, New York, NY, USA, 2012. ACM.
15. Achim J. Stoyanov, Todor and Louloudi, Athanasia and Andreasson, Henrik and Lilienthal. Comparative evaluation of range sensor accuracy in indoor environments. *Proceedings of the 5th European Conference on Mobile Robots, ECMR 2011*, pages 19–24, 2011.

16. P.H.S. Torr and A. Zisserman. Mlesac: A new robust estimator with application to estimating image geometry. *Comput. Vis. Image Underst.*, 78(1):138–156, April 2000.
17. F. Vasconcelos, J.P. Barreto, and U. Nunes. A minimal solution for the extrinsic calibration of a camera and a laser-rangefinder. *IEEE Trans Pattern Anal Mach Intell.*, 34(11):2097–2107, 2012.
18. Z. Zhang. Motion and structure from two perspective views: algorithms, error analysis, and error estimation. 11(5):451–476, 1989.